



Atomic scale patterns formed during surface scanning by atomic force microscopy tips

Omar Teschke, David Mendez Soares, Juracyr Ferraz Valente Filho, and Elizabeth Fátima de Souza

Citation: [Applied Physics Letters](#) **89**, 253125 (2006); doi: 10.1063/1.2423245

View online: <http://dx.doi.org/10.1063/1.2423245>

View Table of Contents: <http://scitation.aip.org/content/aip/journal/apl/89/25?ver=pdfcov>

Published by the [AIP Publishing](#)

Articles you may be interested in

[Enhanced atomic corrugation in dynamic force microscopy—The role of repulsive forces](#)

Appl. Phys. Lett. **100**, 123105 (2012); 10.1063/1.3696039

[Silicon carbide nanotube tips: Promising materials for atomic force microscopy and/or scanning tunneling microscopy](#)

Appl. Phys. Lett. **89**, 123126 (2006); 10.1063/1.2221418

[Nanobubbles on solid surface imaged by atomic force microscopy](#)

J. Vac. Sci. Technol. B **18**, 2573 (2000); 10.1116/1.1289925

[Effect of hydrogen etching on 6H SiC surface morphology studied by reflection high-energy positron diffraction and atomic force microscopy](#)

Appl. Phys. Lett. **76**, 1119 (2000); 10.1063/1.125957

[Influence of electrostatic forces on the investigation of dopant atoms in layered semiconductors by scanning tunneling microscopy/spectroscopy and atomic force microscopy](#)

J. Vac. Sci. Technol. A **15**, 1466 (1997); 10.1116/1.580563



AIP | Journal of
Applied Physics

Journal of Applied Physics is pleased to
announce **André Anders** as its new Editor-in-Chief

Atomic scale patterns formed during surface scanning by atomic force microscopy tips

Omar Teschke,^{a)} David Mendez Soares, and Juracyr Ferraz Valente Filho
Laboratório de NanoEstruturas e Interfaces, Instituto de Física, UNICAMP, 13083-970 Campinas, San Paulo, Brazil

Elizabeth Fátima de Souza
Faculdade de Química, PUC-Campinas, 13012-970 Campinas, San Paulo, Brazil

(Received 27 September 2006; accepted 16 November 2006; published online 22 December 2006)

In this work, tip sliding at the water/substrate interfacial region was used to investigate the pattern observed during image acquisition with atomic resolution in atomic force microscopy. The process responsible for the pattern formation is the oscillatory movement of the tip in the direction that is normal to scanning induced by a change in the water interfacial dielectric permittivity from $\epsilon \approx 4$ at the interface to $\epsilon \approx 80$ (bulk value) that results in a variation of the measured force acting on the tip of ≈ 30 pN. © 2006 American Institute of Physics. [DOI: 10.1063/1.2423245]

The capabilities of scanning force microscopy (SFM) can be exploited in a number of operational modes. The probe tip will respond to in-plane as well as out-of-plane force components.¹ Atomic scale contrast obtained in contact mode images arises supposedly from stick-slip interactions²⁻⁶ that produce symmetries and real space modulations that coincide with those of the surface. However, many groups reported atomic or molecular resolution in lateral force and topography,⁷ but only a few proved to be true atomic/molecular.⁸ In order to explain the observed patterns it is assumed that most of the atomic or molecular resolved SFM measurements are not recorded with a single atomic tip. Multiple tip contacts that are commensurable with the sample lattice structure can unfortunately also provide periodic patterns (Moiré pattern). Here we propose that, associated with the atomic resolution measurements, there is another possible mechanism that generates nanoscale periodicities.

To perform our experiments, we have used a home-built liquid cell and a TopoMetrix TMX 2000 (Ref. 9) commercial atomic force microscope (AFM). The cantilever had a low vertical spring constant of 0.03 N/m that corresponded to a vertical force sensitivity of as low as 3 pN in the present measurements; therefore, there was a comparatively low stiffness along the surface normal (Z) of 0.03 N/m and a high stiffness to lateral spring constant due to the triangular cantilever shape. An etched Si_3N_4 tip was scanned back and forth over a freshly cleaved mica surface immersed in liquid water or air. All the experiments were carried out at room temperature in a closed chamber, in which the relative humidity (RH) is $\sim 60\%$. The applied normal force on the cantilever was held constant at ~ 10 nN, which reduced the thermal vibration from 3.7 to about 0.2 Å.¹⁰

Figure 1 shows a typical forward scan for a mica substrate scanned in air (60% RH) with a scanning speed of 100 nm/s at a 45° angle with the cantilever axis. The lower part of the figure shows a filtered image. Observe that there is a spatial periodicity of ~ 1.86 Å in both scanned directions. This periodicity is not associated with the periodicity of the mica substrate (5.4 Å).¹¹ In order to investigate its

origin we then scanned mica samples in water with a scanning speed of 100 nm/s, but now along the normal direction to the cantilever axis. The result is shown in Fig. 2. Observe that there is a ~ 1.31 Å periodicity only along the scanned direction. The lower part of the figure shows the vertical profile image (VPI), i.e., tip up-and-down movement versus horizontal scanned distance. The measured amplitude of the cantilever oscillations is ~ 10 Å, which corresponds to a factor 50 times larger than the thermal vibration amplitude (~ 0.2 Å). The scanning was repeated for various speeds starting at 5 up to 100 nm/s, and the force versus distance profile was not substantially modified. For scanning speeds higher than 100 nm/s no pattern was observed. A test was performed using tips with distinct elastic stiffness coefficients; the result shows no variation with the cantilever spring constant; consequently, the oscillation is not associated with any natural oscillation frequency of the cantilever.

In order to understand the origin of the up-and-down movement of the tip, let us refer to Fig. 3 that shows a schematic diagram of the electric signal applied to the piezoelectric transducer during scanning. A description of the sweeping digital signal follows. The diagram shows the piezodisplacement that corresponds to the digitalization of the

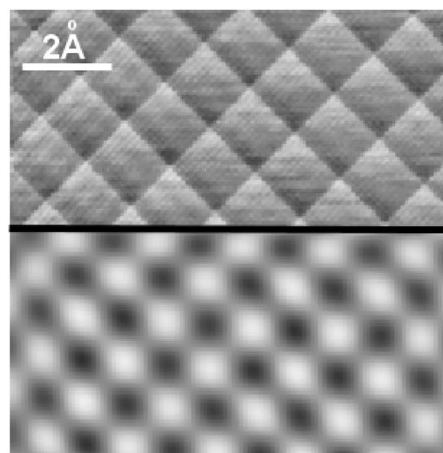


FIG. 1. Mica substrate scanned in air (60% RH) with a scanning speed of 100 nm/s at an angle of 45° with the cantilever axis. The measured periodicity is $1.31 \times 2^{1/2}$ Å for a scanning in both X and Y directions.

^{a)}Electronic mail: oteschke@ifi.unicamp.br

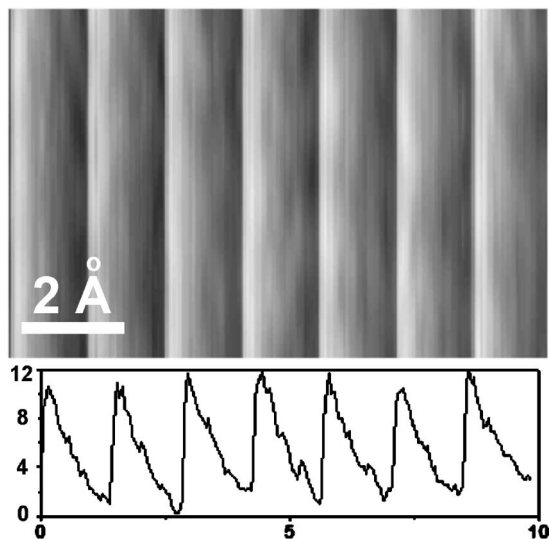


FIG. 2. Mica substrate scanned in water with a scanning speed of 100 nm/s at an angle of 90° with the cantilever axis. The lower part shows the VPI that displays the up-and-down movement (Z axis); the units are given in angstroms and the force acting on the tip is given by k (cantilever spring constant ~ 0.03 N/m) times the Z displacement ~ 1 nm resulting in a force of ~ 30 pN. Inset reproductions of the sliding tip traces obtained during steady-state sliding of tip/water/mica interfaces (Ref. 9). The measured periodicity ~ 1.31 Å.

applied sweep voltage. A staircase potential with voltage steps ΔV corresponds to a spatial periodicity a in the scanning distance. For the model used in this work, an AFM TopoMetrix TMX 2000, a is equal to 1.31 Å. The spatial component displacement patterns may be obtained by Fourier-transforming the staircase function which has components indicated by k , $2k$, and $3k$ where $k=1/a$. There is then a spatial frequency with a periodicity of ~ 1.31 Å for scanning along the X or Y direction and a spatial periodicity of $1.31 \times 2^{1/2}$ for scanning simultaneously the X and Y directions corresponding to a 45° scan with the cantilever axis.

Observe that the scanning velocity is different from zero only at the applied voltage steps (see Fig. 3). Therefore the apparent slip-stick motion of the tip is not the result of the tip

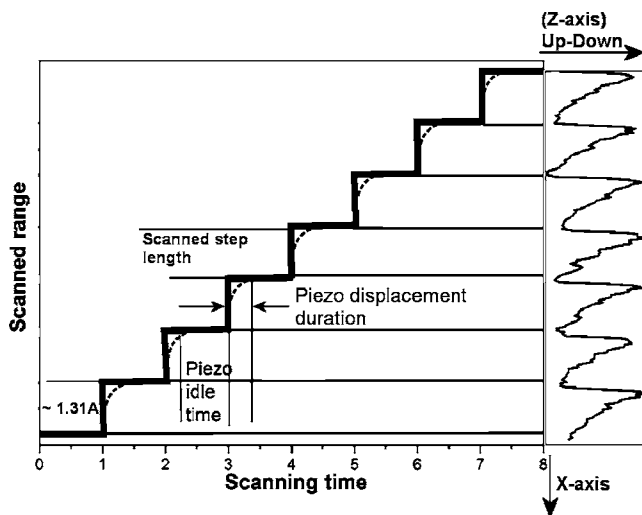


FIG. 3. Schematic diagram of the applied voltage to the scanner as a function of time. The step length comes to 1.31 Å. To the left of the figure the tip displacement normal to the surface direction (z axis) and along the scanned directions (x axis) are displayed.

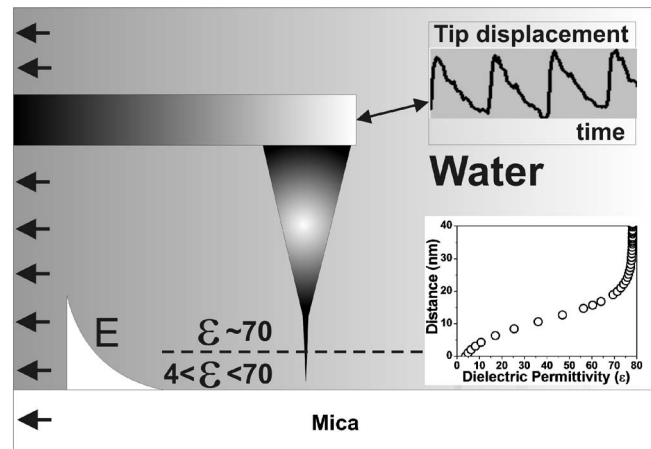


FIG. 4. Scheme of polarization force acting on the tip. The sample is scanned by a triangular shape AFM cantilever where twist variation of the lateral force was not detected and the predominant force acting on the tip results in an up-and-down movement during each scan line. The calculation of the dielectric permittivity profile is given in Ref. 15 and 16.

interaction with the substrate as previously described for other configurations in the literature,¹⁰ but it is the result of the piezoelectric motion imposed by the applied stepped voltage.

The up-and-down tip movement versus distance curve (see the lower inset in Fig. 2) shows two transient responses of the tip to the forced motion imposed by the piezotransducer: The immersion of the tip is associated with the piezo-displacement during the fast step voltage rise time and the tip emersion that occurs between the two steps of the applied voltage. During this time interval the scanner is stationary.

The last question that we are concerned with is the origin of the up-and-down force on the tip. Initially we have estimated the force associated with the liquid drag on the cantilever using the expression from Ref. 12; the value of the drag force on the cantilever for speeds used in this work is calculated to be $\sim 10^{-23}$ N, i.e., approximately 12 orders of magnitude lower than the measured force of $\sim 10^{-11}$ N (see Fig. 2). The measurement that confirms that tip oscillations described in this work are not related to liquid drag is associated with the observation of a similar oscillation amplitude for cantilevers operating in water and in air where the viscosity is $\sim 10^3$ smaller than water which should result in force distinct by a factor of 10^3 , since the drag force is proportional to the kinetic viscosity of the medium. The force has to be associated with their common interaction region, i.e., the liquid between tip and substrate. For a cantilever immersed in water it is possible to calculate the force acting on the tip using our previous work,¹³ where we have shown that there is a dielectric exchange force acting on the tip when the tip is immersed in a mica double layer. It is associated with the exchange of the tip volume with $\epsilon_{\text{tip}} \sim 7$ by the variable ϵ_{water} of the double layer (see Fig. 4). The expression of the force is given by

$$\Delta F_z = -\frac{\epsilon_0}{2} \frac{\partial}{\partial z} \int (\epsilon_{\text{tip}} - \epsilon_{\text{water}}) \bar{E}^2 dv, \quad (1)$$

where the volume (dv) is associated with the immersion of the tip in the mica double layer and z is the normal direction to the mica surface. If we assume that the tip radius is ~ 5 nm, the electric field $|E| = |D|(\epsilon_0 \epsilon_r)^{-1}$, $D \approx 0.6$ C/m², di-

electric constant $\epsilon_r \sim 4$ at the interface, and $\epsilon_r \sim 80$ at the bulk, the force calculated value is ~ 100 pN. For an experimental measured value of ~ 1 nm of the displacement of the tip, shown in Fig. 2, and using a tip stiffness of 0.03 N/m, we obtain a force of ~ 30 pN. This calculated value assumes two states where the first is characterized by $\epsilon_r = 4$ and the second is a disordered state induced by the tip motion with $\epsilon_r = 80$, which gives values higher than the measured value of 30 pN; the difference is probably an indication that the tip movement induces a partial disorder with ϵ values lower than 80. The explanation for the movement of the tip is that while the tip is stationary, the apex of the tip returns to the original height since $\epsilon_{\text{tip}} E^2 > E^2 \epsilon_{\text{water}}$ which corresponds to a water cluster reoriented structure ($\epsilon_r \sim 4$). It remains stationary during the period where the voltage is constant which has to be larger than the water reorientation time, before jumping onward to the next point corresponding to the next voltage step. During the rise time of the voltage step applied to the piezo a relative tip substrate motion and consequently a disordered structure with $\epsilon_r \sim 80$ are induced, and since now $\epsilon_{\text{tip}} E^2 < E^2 \epsilon_{\text{water}}$ the tip is immersed in the double layer. This may be summarized as follows: The switching time of the piezoelectric τ_{ini} has to be much shorter than the confined liquid relaxation time τ_{liquid} , and the duration of the voltage step function $\tau_{\text{step duration}}$ has to be larger than the organization time of the confined liquid, i.e., $\tau_{\text{switch}} \leq \tau_{\text{liquid}} \leq \tau_{\text{step duration}}$. This hypothesis is in agreement with the experimental result that no oscillation is observed for high scanning speed (> 150 nm/s).

In order to modify the amplitude of the spatial components of the observed scanning pattern solutions of $10^{-3} M$ KCl, $10^{-3} M$ NaCl, and $10^{-3} M$ LiCl were used. The effect of adding salt to the solution in the interfacial stationary dielectric permittivity spatial distribution has been previously published.¹⁴ Consequently the immersion and emersion profiles shown in Fig. 2 should be modified, and this was experimentally verified.

In conclusion the pattern observed during image acquisition with atomic resolution in AFM was shown to be generated by an oscillating movement of the tip induced by a

change in the water interfacial dielectric permittivity. The process may be summarized as follows: The melting of the interfacial water structure ($\epsilon_{\text{water}} \approx 80$) is induced by the tip scanning which is followed by a process involving water structure reorientation ($\epsilon_{\text{water}} \approx 4$) between voltage steps (piezotransducer idle time). For $\epsilon_{\text{water}} \approx 80$ the tip is immersed in order to minimize the energy distribution since $\epsilon_{\text{tip}} E^2 < \epsilon_{\text{water}} E^2$, while there is emersion when the tip is stationary. The amplitude of the spatial components of the observed scanning pattern was altered by the addition of salts to the solution which are known to modify the interfacial dielectric permittivity.

The authors are grateful to L. O. Bonugli and J. R. Castro for technical assistance, to CNPq for funding through Grant No. 523.268/95-5, and to FAPESP for the financial support through Grant No. 03/12529-4.

¹C. M. Mate, G. M. McClelland, R. Erlandsson, and S. Chiang, *Phys. Rev. Lett.* **59**, 1942 (1987).

²R. W. Carpick and M. Salmeron, *Chem. Rev. (Washington, D.C.)* **97**, 1163 (1997).

³H. Holscher, U. D. Schwarz, O. Zworner, and R. Wiesendanger, *Phys. Rev. B* **57**, 2477 (1998).

⁴M. Ishikawa, S. Okita, N. Minami, and K. Miura, *Surf. Sci.* **445**, 488 (2000).

⁵H. Holscher, U. D. Schwarz, and R. Wiesendanger, *Europhys. Lett.* **36**, 19 (1996).

⁶K. L. Johnson and J. Woodhouse, *Tribol. Lett.* **5**, 155 (1998).

⁷H. Takano and M. Fujihira, *J. Vac. Sci. Technol. B* **14**, 1272, (1996).

⁸R. M. Overney, H. Takano, M. Fujihira, W. Paulus, and H. Ringsdorf, *Phys. Rev. Lett.* **72**, 3546 (1994).

⁹O. Teschke and E. F. Souza, *Rev. Sci. Instrum.* **69**, 3588 (1998).

¹⁰E. Meyar, R. M. Overney, K. Dransfeld, and T. Gyalog, *Nanoscience* (World Scientific, Singapore, 2002), Chap. 9, 337.

¹¹E. F. de Souza, R. A. Douglas, and O. Teschke, *Langmuir* **13**, 6012 (1997).

¹²O. Teschke, R. A. Douglas, and T. A. Prolla, *Appl. Phys. Lett.* **70**, 1977 (1997).

¹³O. Teschke, G. Ceotto, and E. F. de Souza, *Appl. Phys. Lett.* **78**, 3064 (2001).

¹⁴O. Teschke and E. F. de Souza, *Phys. Chem. Chem. Phys.* **7**, 3856 (2005).

¹⁵O. Teschke, G. Ceotto, and E. F. de Souza, *Chem. Phys. Lett.* **326**, 328 (2000).

¹⁶O. Teschke and E. F. de Souza, *Chem. Phys. Lett.* **403**, 95 (2005).